

A Novel Riesz Transforms based Coding Scheme for Finger-Knuckle-Print Recognition

Lin Zhang, Hongyu Li
School of Software Engineering
Tongji University
Shanghai, China
{cslinzhang, hyl}@tongji.edu.cn

Ying Shen
Dept. Computer Science
City University of Hong Kong
Hong Kong, China
csyingshen@gmail.com

Abstract—It is well recognized that in biometric systems feature extraction and representation are key considerations. Among various feature extraction and representation schemes, coding-based methods are most attractive because they have the merits of high accuracy, robustness, compactness and high matching speed, and thus they have been adopted in many different kinds of biometric systems, such as iris, palmprint, and finger-knuckle-print (FKP) systems. However, how to devise a good coding scheme for FKP recognition is still an open issue. In this paper, based on the finding that Riesz transforms can well characterize the visual patterns, we propose to encode the local patches of an FKP image by using 2nd-order Riesz transforms. Specifically, we propose a 6-bits coding scheme, namely RieszCompCode, which consists of 6 bit-planes. In RieszCompCode, three of the bit-planes are obtained by binarizing the image's responses to the three 2nd-order Riesz transforms, and the other three ones are from the classical CompCode scheme. Experiments conducted on the benchmark PolyU FKP database corroborate that the proposed RieszComopCode can surpass all the other coding schemes evaluated for FKP verification in terms of verification accuracy.

Keywords—finger-knuckle-print; Riesz transform; biometrics

I. INTRODUCTION

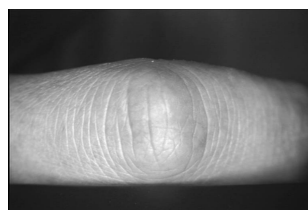
Recognizing the identity of a person with high confidence is a critical issue in various applications, such as e-banking, access control, passenger clearance, national ID card, etc. The need for reliable user authentication techniques has significantly increased in the wake of heightened concerns about security, and rapid advancement in networking, communication and mobility [1]. Biometrics based methods, which use unique physical or behavioral characteristics of human beings, are of broad interest and have great potentials because of their high accuracy and convenience to use in the modern e-world. In fact, researchers have exhaustively investigated a number of different biometric identifiers, including fingerprint, face, iris, palmprint, hand geometry, voice, and gait, etc [2].

Recently, scholars have reported that finger-knuckle-print (FKP), the image pattern of skin folds and creases in the outer finger knuckle surface, is highly unique and can serve as a distinctive biometric identifier [3-9]. Compared with fingerprint, a traditional hand-based biometric trait, FKP is hard to be abraded since people hold stuffs with the inner side

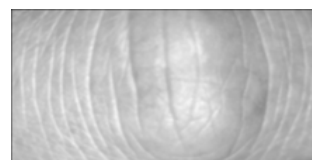
of the hand. In addition, unlike fingerprint, there is no stigma of criminal investigation associated with the finger knuckle surface, so FKP can have a higher user acceptance rate [4]. Moreover, people rarely leave FKP remains on the stuff surface, making the loss of private data less possible. Thus, FKP has a great potential to turn into a widely accepted biometric identifier.



(a)



(b)



(c)

Figure 1. (a) Outlook of the PolyU FKP recognition system; (b) a typical FKP image taken from the PolyU FKP database [7]; (c) the cropped ROI image from the original FKP image shown in (b).

In Zhang *et al.*'s works [3-7], a novel online FKP-based personal authentication system has been established. It comprises four major components: FKP image acquisition, ROI (region of interest) extraction, feature extraction and feature matching [3]. Fig. 1a shows the outlook of their FKP recognition system and Fig. 1b shows a typical FKP image taken from the PolyU FKP database [7] which is now public available. Fig. 1c shows the extracted ROI image using the ROI extraction algorithm presented in [3]. The later feature extraction and matching are based on the extracted ROIs.

As in many pattern classification tasks, feature extraction and matching plays a key role in FKP-based personal

authentication systems. To this end, researchers have proposed several different methods. In [5], Zhang *et al.* used the Gabor filter based competitive coding scheme, which was originally designed for palmprint recognition [10], to extract the local dominant orientation as FKP features. In [3], Zhang *et al.* combined the orientation information and the magnitude information extracted by Gabor filters. In [6], the Fourier transform coefficients of the image were taken as the feature and the band-limited phase-only correlation (BLPOC) technique [11] was employed to calculate the similarity between two sets of Fourier transform coefficients. In the local-global information combination (LGIC) feature extraction scheme [4], the local orientation extracted by the Gabor filters is taken as the local feature while the Fourier coefficients are taken as a global feature. In [8], Morales *et al.* used a real Gabor filter to enhance the FKP image and then used the scale invariant feature transform (SIFT) to extract features.

In this paper, we focus on designing effective and efficient algorithms for feature extraction and matching of FKP images. When designing feature extraction and matching methods, several key factors need to be considered, such as the computation complexity for the feature extraction, the obtained feature length, the matching speed, and the recognition accuracy, etc. By taking these factors into consideration, usually coding-based approaches are superior to the other kinds of methods. Generally speaking, they have the merits of short feature length, less parameters to adjust, high accuracy, robustness to illumination variation and fast feature extraction and matching speed. In a typical coding-based feature extraction method, each field of the code map is assigned as a bit-wise code, based on the quantization of the image's responses to a set of filters. Coding based methods are largely inspired by the great success of the IrisCode invented by Daugman [12] for iris recognition. Daugman has demonstrated that the real-time brute-force identification in large databases is possible with coding based features and the associated bit-wise Hamming distance based matching. Now in addition to the IrisCode, several different coding methods have also been successfully developed for palmprint recognition [10, 13, 14] and FKP recognition [3, 5].

How to devise highly effective and efficient coding schemes for FKP recognition is still an open issue and requires further investigation. Recent studies in image processing and applied mathematics have shown that local image features can be well represented and extracted with Riesz transforms in a unified framework [15-23]. Thus, it can be expected that coding schemes derived from Riesz transforms can have good characteristics. Riesz transform has already been used in some image processing applications, such as the local structure analysis [16, 20, 21], the image quality assessment [22], the texture classification [23], etc. And the studies have also shown that 2nd-order Riesz transforms are more capable in characterizing the image local structures, especially the i2D (intrinsic two dimensional) image features, than the 1st-order Riesz transforms [20, 21]. Based on these considerations, in this paper, we propose to quantify the image's responses to the 2nd-order Riesz transforms to devise a new 6-bits coding scheme, namely RieszCompCode. Specially, three bit-planes of RieszCompCode are obtained by binarizing the image's

responses to the three 2nd-order Riesz transforms and the other three ones are from the classical CompCode (competitive coding) scheme [3, 5]. Extensive experiments conducted on the benchmark PolyU FKP database [7] demonstrate that RieszCompCode can achieve much higher verification accuracy than all the other state-of-the-art coding based FKP verification methods.

The remainder of this paper is organized as follows. Section II introduces the related work. Section III presents the proposed RieszCompCode coding scheme. Section IV reports the experimental results. Conclusions are presented in Section V.

II. RELATED WORK

In this section, some background material related to our work will be briefly reviewed, including the Riesz transforms and the CompCode scheme.

A. Riesz Transforms

The Hilbert transform based analytic signal, first proposed by Denis Gabor [24], is a powerful tool for the 1D real signal analysis. The advantage of the 1D analytic signal is that it allows one to obtain the time-varying amplitude and phase of a 1D signal. After its birth, the analytic signal has been utilized in various applications, where amplitude or frequency modulation is involved, e.g. [25].

In the literature, there are many attempts reported to generalize the 1D analytic signal to the 2D case and among them, the monogenic signal [15] proposed by Felsberg and Sommer is the most distinguished one. The monogenic signal is build upon the 1st-order Riesz transform which is a vector-valued extension of the classical Hilbert transform [26]. The convolution kernels of the Riesz transform in the nD spatial domain can be expressed as

$$R_j(\mathbf{y}) = c_n \frac{\mathbf{y}_j}{|\mathbf{y}|^{n+1}} \quad (1)$$

where $c_n = \Gamma[(n+1)/2]/\pi^{(n+1)/2}$, $\mathbf{y} = (y_1, y_2, \dots, y_n)$ and $j = 1, 2, \dots, n$. In 2D, which is the case of interest for image processing applications (in this case, $n = 2$, $j = \{1, 2\}$, and $c_n = 1/2\pi$), the Riesz transform consists of two kernels expressed as

$$h_x(\mathbf{x}) = \frac{x}{2\pi|\mathbf{x}|^3}, h_y(\mathbf{x}) = \frac{y}{2\pi|\mathbf{x}|^3} \quad (2)$$

where $\mathbf{x} = (x, y) \in \mathbb{R}^2$. The Fourier transforms of h_x and h_y are

$$H_u(\mathbf{u}) = -j \frac{u}{|\mathbf{u}|}, H_v(\mathbf{u}) = -j \frac{v}{|\mathbf{u}|} \quad (3)$$

where $\mathbf{u} = (u, v) \in \mathbb{R}^2$. Given a 2D signal $f(\mathbf{x})$, its corresponding monogenic signal $f_M(\mathbf{x})$ is defined as the combination of the original signal itself and its two Riesz transforms

$$f_M(\mathbf{x}) = (f(\mathbf{x}), h_x\{f\}(\mathbf{x}), h_y\{f\}(\mathbf{x})) \quad (4)$$

where $h_x\{f\}$ means convolving f with h_x . As the Riesz transform with respect to the Hilbert transform, the monogenic signal is a multi-dimensional isotropic generalization of the 1D analytic signal.

However, theoretically speaking, the 1st-order Riesz transform based monogenic signal only enables the rotationally invariant analysis of i1D structures, such as edges and lines. In order to characterize i2D image structures, e.g., corners and junctions, higher order Riesz transforms need to be exploited [20, 21]. In this paper, we only consider 2nd-order Riesz transforms. Given an image $f(\mathbf{x})$, the three 2nd-order Riesz transforms of f are defined as

$$\begin{aligned} h_{xx}\{f\}(\mathbf{x}) &\equiv h_x\{h_x\{f\}\}(\mathbf{x}) \\ h_{xy}\{f\}(\mathbf{x}) &\equiv h_x\{h_y\{f\}\}(\mathbf{x}) \\ h_{yy}\{f\}(\mathbf{x}) &\equiv h_y\{h_y\{f\}\}(\mathbf{x}) \end{aligned} \quad (5)$$

Using the convolution theorem, the transfer functions of h_{xx} , h_{xy} , and h_{yy} in the Fourier domain are

$$\begin{aligned} H_{uu}(\mathbf{u}) &\equiv \left(-j \frac{u}{\sqrt{u^2 + v^2}}\right) \left(-j \frac{u}{\sqrt{u^2 + v^2}}\right) = -\frac{u^2}{u^2 + v^2} \\ H_{uv}(\mathbf{u}) &\equiv \left(-j \frac{u}{\sqrt{u^2 + v^2}}\right) \left(-j \frac{v}{\sqrt{u^2 + v^2}}\right) = -\frac{uv}{u^2 + v^2} \\ H_{vv}(\mathbf{u}) &\equiv \left(-j \frac{v}{\sqrt{u^2 + v^2}}\right) \left(-j \frac{v}{\sqrt{u^2 + v^2}}\right) = -\frac{v^2}{u^2 + v^2} \end{aligned} \quad (6)$$

B. CompCode

CompCode was originally designed for palmprint recognition [10], and later it was adapted for FKP recognition [3, 5]. 2D Gabor filters, which are defined as follows, are used in CompCode:

$$G(x, y) = \exp\left(-\frac{1}{2}\left(\frac{x'^2}{\sigma_x^2} + \frac{y'^2}{\sigma_y^2}\right)\right) \cdot \cos\left(\frac{2\pi}{\lambda}x'\right) \quad (7)$$

where $x' = x\cos\theta + y\sin\theta$ and $y' = -x\sin\theta + y\cos\theta$. In Eq. (7), λ represents the wavelength of the sinusoidal factor, θ represents the orientation of the normal to the parallel stripes of the Gabor function, σ_x and σ_y are the standard deviations of the 2D Gaussian envelop. Denote by G_R the real part of the Gabor filter G . With six G_R s sharing the same parameters, except the parameter of orientation, the local orientation information of the image f at the position (x, y) can be extracted and coded. Mathematically, this competitive coding process can be expressed as

$$\text{CompCode}(x, y) = \arg \min_j \{f(x, y) * G_R(x, y, \theta_j)\} \quad (8)$$

where $*$ stands for the convolution operation, $\theta_j = j\pi/J$, $j = \{0, \dots, J-1\}$ and J represents the number of orientations. Usually, J is set as 6, which has been proved to be an appropriate choice both theoretically [27] and experimentally [3, 5, 10]. Then, the dominant orientation $\{0, \pi/6, \pi/3, \pi/2, 2\pi/3, 5\pi/6\}$ will be encoded with three bits as $\{000, 001, 011, 111, 110, 100\}$ for efficient representation and bitwise matching.

III. RIESZCOMPCODE

In this section, our proposed coding scheme RieszCompCode will be presented. It can be seen that the key difference between different coding schemes is that they adopt

different filters and the coding scheme largely depends on the design of the filters adopted. When designing a new coding scheme, it is highly desired that the selected filters can well characterize the intrinsic structure of the image local patch and has a strong discriminating power. On the other hand, recent studies have been shown that 2nd-order Riesz transform is a powerful tool to represent i2D image features. Thus, good verification performance can be expected if the new coding scheme is based on 2nd-order Riesz transforms.

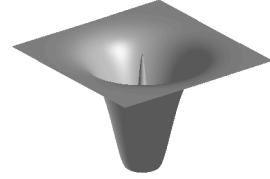


Figure 2. An example of the LOP filter in the frequency domain.

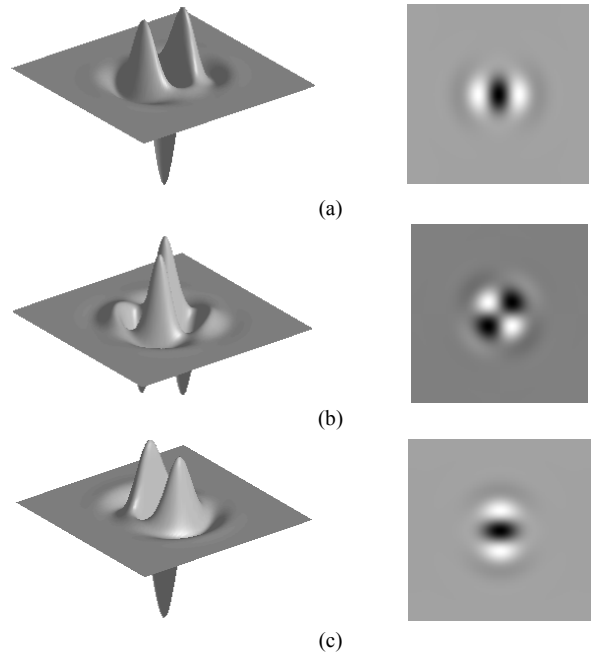


Figure 3. Shapes of the band-pass filtered 2nd-order Riesz transform filters in the spatial domain. For each filter, its shape is shown both in 3D surface format and in image format. (a) $h_{xx}\{h_{LOP}\}$; (b) $h_{xy}\{h_{LOP}\}$; and (c) $h_{yy}\{h_{LOP}\}$.

Riesz transforms based image analysis assumes that the signal consists of few frequencies, or in other words, it is band limited. However, real images usually consist of a wide range of frequencies. Therefore, it is necessary to pre-filter the image with a chosen band-pass filter before applying the Riesz transform to it. Based on the associative property of the convolution operation, we can apply the Riesz transforms to the chosen band-pass filter and then to filter the image with these new filters. With respect to the band-pass filter, we use the Laplacian of Poisson (LOP) filter h_{LOP} proposed in [20], whose transfer function in the Fourier domain is

$$H_{LOP}(\mathbf{u}) = -4\pi^2 |\mathbf{u}|^2 \exp(-2\pi |\mathbf{u}| s), \mathbf{u} \in \mathbb{R}^2 \quad (9)$$

where s is used to control the center frequency. Compared with the other commonly used band-pass filters, such as the Gabor

filter or the log-Gabor filter, the advantage of LOP is that it has only one parameter to adjust. An example of the LOP filter with $s = 3.5$ in the Fourier domain is shown in Fig. 2.

We apply the filters $h_{xx}\{h_{LOP}\}$, $h_{xy}\{h_{LOP}\}$ and $h_{yy}\{h_{LOP}\}$ to the image to get its responses to the 2nd-order Riesz transforms after a band-pass filtering. In the Fourier domain, the transfer functions of $h_{xx}\{h_{LOP}\}$, $h_{xy}\{h_{LOP}\}$ and $h_{yy}\{h_{LOP}\}$ can be expressed as $H_{LOP}H_{uu}$, $H_{LOP}H_{uv}$, and $H_{LOP}H_{vv}$. Shapes of these filters (with a specific s) in the spatial domain are shown in Fig. 3.

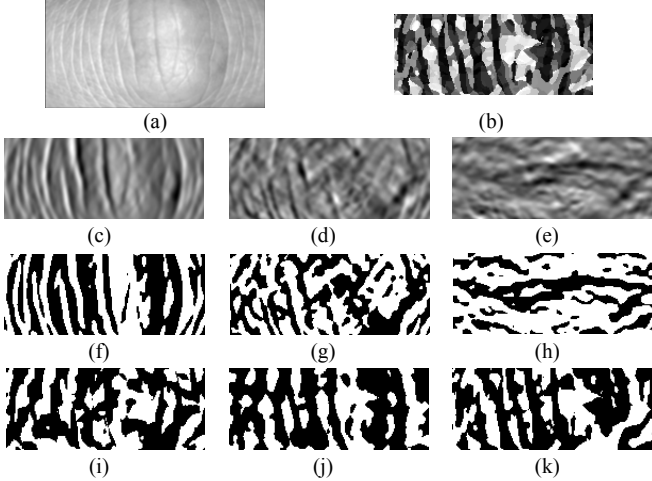


Figure 4. Illustration for the computation of RieszCompCode for a given FKP image. (a) an FKP ROI image f ; (b) the extracted 6-bits RieszCompCode map; (c) ~ (e) are f 's responses to $h_{xx}\{h_{LOP}\}$, $h_{xy}\{h_{LOP}\}$, and $h_{yy}\{h_{LOP}\}$, respectively; (f) ~ (h) are binarized from (c) ~ (e), respectively; (i) ~ (k) are the three bit-planes extracted from f by using the CompCode scheme.

Theoretically speaking, we can directly match two images based on their raw responses to the filters $h_{xx}\{h_{LOP}\}$, $h_{xy}\{h_{LOP}\}$ and $h_{yy}\{h_{LOP}\}$. However, that will lead to a large feature size for storage and a high computational complexity for matching. Hence instead, we design a new coding scheme based on these responses. Specifically, given an image $f(\mathbf{x})$, we can get three bits for each position \mathbf{x} by binarizing $h_{xx}\{h_{LOP}\{f\}\}(\mathbf{x})$, $h_{xy}\{h_{LOP}\{f\}\}(\mathbf{x})$, and $h_{yy}\{h_{LOP}\{f\}\}(\mathbf{x})$ according to their signs. On the other hand, CompCode is another effective coding based feature extraction method and it depends on local dominant orientation information of the examined image, so it can provide complementary discriminating power to the code bits obtained from Riesz transforms. Thus, in order to pursue higher verification accuracy, in our coding scheme, we combined the three bits obtained from the image's 2nd-order Riesz transforms and the three bits obtained from the CompCode scheme. We name such a coding scheme as RieszCompCode. It is obvious that each RieszCompCode(\mathbf{x}) comprises 6-bits. The computation process of RieszCompCode is illustrated in Fig. 4 using a sample FKP image taken from [7]. Fig. 4(a) is an FKP ROI image f ; Fig. 4(b) is the extracted 6-bits RieszCompCode map; Figs. 4(c) ~ 4(e) are f 's responses to $h_{xx}\{h_{LOP}\}$, $h_{xy}\{h_{LOP}\}$, and $h_{yy}\{h_{LOP}\}$, respectively; Figs. 4(f) ~ 4(h) are binarized from 4(c) ~ 4(e), respectively; Figs. 4(i) ~ 4(k) are the three bit-planes extracted from f by using the CompCode scheme.

Consider two RieszCompCode maps, P and Q . $P_1(Q_1)$, $P_2(Q_2)$, $P_3(Q_3)$, $P_4(Q_4)$, $P_5(Q_5)$, and $P_6(Q_6)$ are six bit-planes of P (Q). Then, we adopt the normalized Hamming distance to measure the dissimilarity between P and Q as

$$d(P, Q) = \frac{\sum_{y=1}^{Rows} \sum_{x=1}^{Cols} \sum_{i=1}^6 P_i(x, y) \otimes Q_i(x, y)}{6S} \quad (10)$$

where S is the area of the code map, and \otimes represents the bitwise “exclusive OR” operation.

In practice, taking into account the possible translations in the extracted ROI sub-image with respect to the one extracted in the enrolment, multiple matches are performed by translating one set of features in horizontal and vertical directions. And the minimum of the resulting matching distances is considered to be the final matching distance. In such cases, S is the area of the overlapping parts of the two code maps.

IV. EXPERIMENTAL RESULTS

A. Database and Test Protocol

In order to validate the effectiveness and the efficiency of the proposed RieszCompCode scheme, we conducted experiments and comparisons on the established FKP database, which is available at [7]. FKP images were collected from 165 volunteers in two separate sessions. In each session, the subject was asked to provide 6 images for each of the left index finger, the left middle finger, the right index and the right middle finger. In total, the database contains 7,920 images from 660 different fingers. In our experiments, we took images collected at the first session as the gallery set and images collected at the second session as the probe set. To obtain statistical results, each image in the probe set was matched with all the images in the gallery set. If the two images were from the same finger, the matching between them was counted as a genuine matching; otherwise it was counted as an imposter matching. The equal error rate (EER) (the point where the false accept rate (FAR) is equal to the false reject rate (FRR)) was used to evaluate the verification accuracy. Besides, by adjusting the matching threshold, a detection error tradeoff (DET) curve [28], which is a plot of false reject rate (FRR) against false accept rate (FAR) for all possible thresholds, can be created. The DET curve can reflect the overall verification accuracy of a biometric system. Thus, the DET curve obtained by using each evaluated method will also be provided.

B. Determination of Parameters

In real implementation, parameters need to be determined for RieszCompCode scheme. To this end, we tuned the parameters based on a sub-dataset, which contained the first 300 FKP classes. The tuning criterion was that parameter values that could lead to a lower EER would be chosen. As a result, the parameters used for RieszCompCode were set as: $\sigma_x = 5.0$, $\sigma_y = 9.0$, $\lambda = 23$, and $s = 5.1$ in this paper.

C. FKP Verification Results

Verification aims to answer the question of “whether the person is the one he/she claims to be”. In this experiment, all

the classes of FKPs were involved. Therefore, there were 660 (165×4) classes and 3960 (660×6) images in the gallery set and the probe set each. Each image in the probe set was matched against all the images in the gallery set. Thus, the numbers of genuine matchings and imposter matchings were 23,760 and 15,657,840, respectively.

TABLE I. FKP VERIFICATION PERFORMANCE OF DIFFERENT SCHEMES

	EER (%)
CompCode [3]	1.66
RLOC [14]	1.91
BOCV [13]	1.82
ImCompCode&MagCode [3]	1.48
RieszCompCode	1.26

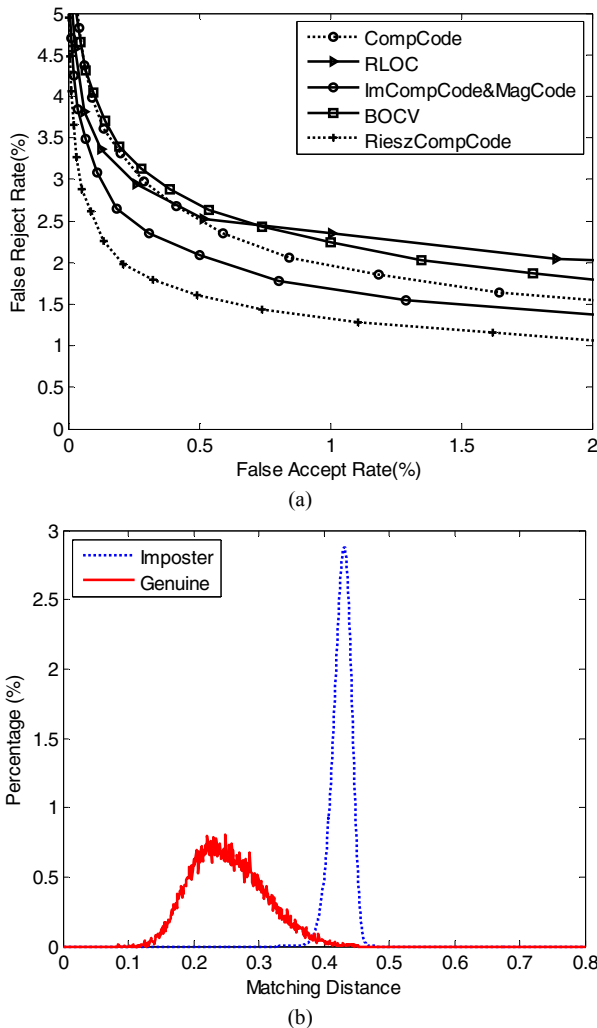


Figure 5. (a) DET curves obtained by the five coding-based FKP verification methods on the PolyU FKP database [7]; (b) distance distributions of genuine matchings and imposter matchings obtained by the proposed RieszCompCode scheme.

For comparison, we compared the proposed RieszCompCode with four other state-of-the-art coding-based feature extraction methods, including CompCode [3], ImCompCode&MagCode [3], RLOC [14], and BOCV [13].

The verification results in terms of EER are summarized in Table I. DET curves obtained by the five evaluated methods are shown in Fig. 5(a). From the EERs listed in Table I and DET curves shown in Fig. 5(a), it can be seen that the newly proposed coding scheme RieszCompCode can achieve much higher verification accuracy than the other coding methods evaluated. The EER obtained by RieszCompCode was 1.26% on PolyU FKP database. Fig. 5(b) shows the distance distributions of genuine matchings and imposter matchings obtained by RieszCompCode.

In implementation, all the convolutions were accomplished via the FFT. The software for RieszCompCode was implemented with Visual C# 2005 on a Dell Inspiron 530s PC embedded Intel 6550 processor and 2GB RAM. With our implementation, for RieszCompCode, the time cost for one feature extraction was about 62.1ms, and the time cost for one feature matching was about 1.4ms. So, it can be seen that RieszCompCode is fast enough for real-time applications.

V. CONCLUSION

Recent studies have shown that Riesz transforms can capture the local image structures powerfully. In this paper, we introduced them into the biometrics community by proposing a novel coding-based feature extraction method for finger-knuckle-print recognition, namely RieszCompCode. RieszCompCode consists of six bit-planes, three of which are from the image's responses to the 2nd-order Riesz transforms and the other three ones are from the classical CompCode scheme. Hence, RieszCompCode integrates the advantages of Riesz transform and CompCode in characterizing the local image features together. At the matching stage, the normalized Hamming distance is employed. Performances of the proposed coding scheme was evaluated and compared with the other four state-of-the-art coding-based methods on the public PolyU FKP database. Experimental results demonstrated that RieszCompCode performs the best in terms of verification accuracy among all the methods evaluated. The EER obtained by RieszCompCode is 1.26%. In addition, RieszCompCode is fast enough and thus can be deployed for real-time applications.

ACKNOWLEDGEMENT

This research was partially supported by National Natural Science Foundation of China under Grant 60903120 and Shanghai Natural Science Foundation of China under Grant 09ZR1434400.

REFERENCES

- [1] A.K. Jain, P.J. Flynn, and A. Ross, Handbook of Biometrics, Springer, 2007.
- [2] S.Z. Li (Ed.), Encyclopedia of Biometrics, Springer, 2009.
- [3] L. Zhang, L. Zhang, D. Zhang, and H. Zhu, "Online finger-knuckle-print verification for personal authentication", Pattern Recognition, vol. 43, pp. 2560-2571, 2010.
- [4] L. Zhang, L. Zhang, D. Zhang, and H. Zhu, "Ensemble of local and global information for finger-knuckle-print recognition", Pattern Recognition, vol. 44, pp. 1990-1998, 2011.

- [5] L. Zhang, L. Zhang, and D. Zhang, "Finger-knuckle-print: a new biometric identifier", ICIP' 09, 2009.
- [6] L. Zhang, L. Zhang, and D. Zhang, "Finger-knuckle-print verification based on band-limited phase-only correlation", CAIP' 09, 2009.
- [7] PolyU FKP Database, 2010. <http://www.comp.polyu.edu.hk/~biometrics>.
- [8] A. Morales, C.M. Travieso, M.A. Ferrer, and J.B. Alonso, "Improved finger-knuckle-print authentication based on orientation enhancement", Electronics Letters, vol. 47, pp. 380-381, 2011.
- [9] D.L. Woodard and P.J. Flynn, "Finger surface as a biometric identifier", Computer Vision and Image Understanding, vol. 100, pp. 357-384, 2005.
- [10] A. Kong and D. Zhang, "Competitive coding scheme for palmprint verification", ICPR' 04, 2004.
- [11] C.D. Kuglin and D.C. Hines, "The phase correlation image alignment method", Int' Conf. Cybernetics and Society, 1975.
- [12] J.G. Daugman, "High confidence visual recognition of persons by a test of statistical independence", IEEE Trans. Pattern Anal. Mach. Intell., vol. 15, pp. 1148-1161, 1993.
- [13] Z. Guo, D. Zhang, L. Zhang, and W. Zuo, "Palmprint verification using binary orientation co-occurrence vector", Pattern Recognition Letters, vol. 30, pp. 1219-1227, 2009.
- [14] W. Jia, D. Huang, and D. Zhang, "Palmprint verification based on robust line orientation code", Pattern Recognition, vol. 41, pp. 1504-1513, 2008.
- [15] M. Felsberg and G. Sommer, "The monogenic signal", IEEE Trans. Signal Process., vol. 49, pp. 3136-3144, 2001.
- [16] M. Felsberg and G. Sommer, "The monogenic scale-space: a unifying approach to phase-based image processing in scale space", J. Math. Imaging and Vision, vol. 21, pp. 5-26, 2004.
- [17] S. Held, M. Storath, P. Massopust, and B. Forster, "Steerable wavelet frames based on the Riesz transform", IEEE Trans. Image Process., vol. 19, pp. 653-667, 2010.
- [18] M. Unser, D. Sage, and D.V.D. Ville, "Multiresolution monogenic signal analysis using the Riesz-Laplace wavelet transform", IEEE Trans. Image Process., vol. 18, pp. 2402-2418, 2009.
- [19] M. Unser and D.V.D. Ville, "Wavelet steerability and the higher-order Riesz transform", IEEE Trans. Image Process., vol. 19, pp. 636-652, 2010.
- [20] A. Sedlazeck, "Local feature detection by higher order Riesz transforms on images", Thesis, University of Kiel, 2008.
- [21] L. Wietzke and G. Sommer, "The signal multi-vector", J. Math. Imaging and Vision, vol. 37, pp. 132-150, 2010.
- [22] L. Zhang, L. Zhang, and X. Mou, "RFSIM: a feature based image quality assessment metric using Riesz transforms", ICIP' 10, 2010.
- [23] L. Zhang, L. Zhang, Z. Guo, and D. Zhang, "Monogenic-LBP: a new approach for rotation invariant texture classification", ICIP' 10, 2010.
- [24] D. Gabor, "Theory of communication", J. Inst. Elec. Eng., vol. 93, pp. 429-457, 1946.
- [25] L. Moura and P. Monteiro, "Design method for FIR-based Hilbert transform filters suitable for broadband AM-SSB", Electronics Letters, vol. 38, pp. 605-606, 2002.
- [26] E. Stein and G. Weiss, Introduction to Fourier Analysis on Euclidean Spaces, Princeton, NJ: Princeton Univ. Press, 1971.
- [27] T.S. Lee, "Image representation using 2D Gabor wavelet", IEEE Trans. Pattern Anal. Mach. Intell., vol. 18, pp. 957-971, 1996.
- [28] A. Martin, G. Doddington, T. Kamm, M. Ordowski, and M. Przybocki, "The DET curve in assessment of detection task performance", Eurospeech' 97, 1997.